IEICE Electronics Express, Vol.16, No.11, 1–6

LETTER

Impacts of phase-locked loop bandwidth on millimeter wave three-dimensional imaging system

Chunhui Fang[1,2], **Wenmin Yu**[1,2], **Yukun Zhu**[1], **Liang Wu**[1], **Tianyu Pen**[1,2], **and Xiaowei Sun**[1a)]

Abstract Signal-to-noise ratio (SNR) of the millimeter wave (MMW) three-dimensional (3D) imaging system plays a critical role in the imaging quality. The impacts of phase-locked loop (PLL) bandwidth on SNR of the imaging system is demonstrated and the relationship between SNR and imaging resolution is analyzed in this paper. Analytical and experimental results show that choosing the optimum PLL loop bandwidth can maximize the SNR and greatly improve the performance of MMW imaging system.

Keywords: PLL, loop bandwidth, phase noise, SNR, MMW imaging
Classification: Microwave and millimeter-wave devices, circuits, and modules

1. Introduction

MMW imaging systems have been widely used for concealed weapon detection at security checkpoints during the recent years [1, 2, 3, 4]. Practical application of these systems needs to be improved [5]. For a better imaging resolution, a higher frequency and a wider bandwidth of transmitting signals have been employed in imaging system among recent researches [6, 7]. When the operation frequency of the imaging system is determined, one effective way to improve imaging resolution is to promote the noise performance and the SNR of the imaging system.

One dominant noise source in MMW imaging system is phase noise of frequency source [5]. The common method to acquire high frequency source with wideband frequency is PLL frequency synthesis [8]. Therefore, it's very important to analyze the impacts of loop bandwidth of PLL on SNR of the imaging system and optimize the loop bandwidth for a relatively higher resolution.

This paper proposes an original method to choose optimum loop bandwidth of PLL for a higher SNR of imaging system and a better imaging resolution. The remainder of this paper is organized as follows. Section 2 briefly introduces the simplified structure of MMW imaging system. In section 3, the phase noise model of PLL is built and the impacts of loop bandwidth on SNR of imaging system are also analyzed. Section 4 demonstrates the impacts of SNR of system on imaging performance. Finally, conclusion is made in section 5.

2. The structure of MMW imaging system

A typical simplified structure of the commercial MMW imaging system and the photograph of the transceiver are shown in Fig. 1. These systems use mechanical scanning to reduce the cost and complication of making two-dimensional arrays [9, 10]. The imaging system mainly includes MMW transceiver front-end and signal processing unit.

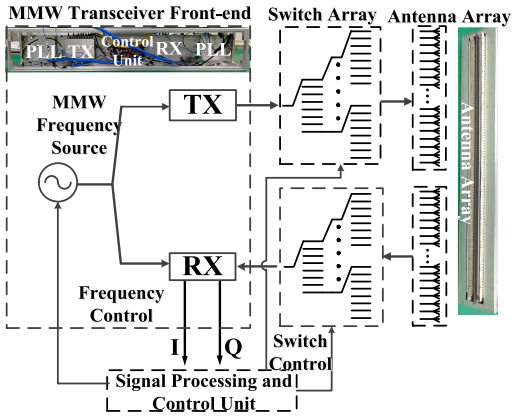

Fig. 1. The simplified structure of MMW imaging system.

The detailed schematic diagram of MMW transceiver front-end is described in Fig. 2.

The radio frequency (RF) source generates wideband frequency signals (in this case from 28 to 33 GHz), which are emitted to detect the targets by transmitting antenna array. The signals reflected by the targets are mixed with local oscillator (LO) signals to get the receiving intermediate frequency (IF) signals (in this case 800 MHz). The IF reference signals (at 800 MHz) are achieved by mixing the coupled signals from RF and LO frequency source. The in-phase (I) and quadrature (Q) signals which contain the amplitude and phase information of scatter signals are obtained by mixing (by I-Q mixer) the IF received signals with IF reference signals. The phase and amplitude information of scatter signal can be theoretically calculated as [10].

$$I + jQ = Ae^{-j2kR} \tag{1}$$

[1]Key Laboratory of Terahertz Solid-State Technology of Chinese Academy of Sciences, Shanghai Institute of Microsystem and Information Technology, Shanghai 200050, China
[2]University of Chinese Academy of Sciences, Beijing 100049, China
a) xwsun@mail.sim.ac.cn

DOI: 10.1587/elex.16.20190187
Received March 20, 2019
Accepted April 24, 2019
Publicized May 17, 2019
Copyedited June 10, 2019

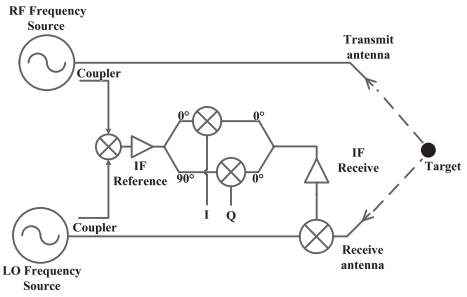

Fig. 2. The schematic diagram of MMW transceiver front-end.

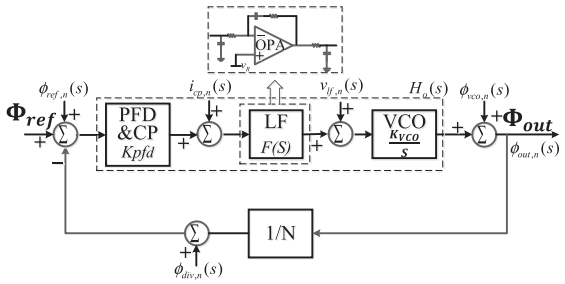

Fig. 3. The linear phase noise model of PLL.

Where A is the amplitude of the scattered signal, R is the range of the target and k is wavenumber. Then the obtained I and Q signals are digitized by highspeed analog to digital converter (ADC), and finally the image-reconstruction algorithm is applied to rebuild the MMW images.

The imaging resolution is mainly dependent on the frequency and bandwidth of the transmitting signals [4, 10]. Once the frequency is selected, an effective method to raise resolution is to increase SNR of the system. In most cases, the RF and LO signals of imaging system are obtained by multiplying the signals from low frequency source, which causes much degeneration of phase noise. Therefore, the phase noise introduced by MMW frequency source is one of the main noise sources of imaging system. The commonly used frequency source is PLL frequency synthesizer due to its good performance of phase noise and spurious suppression. The loop bandwidth is one of the most important parameters of PLL, which determines the performance of PLL in a large degree. Therefore, it's very meaningful to research the relation between the loop bandwidth of PLL and the performance of imaging system.

3. PLL phase noise model and the impacts of loop bandwidth on imaging system SNR

3.1 Modeling of charge pump PLL phase noise

Each component in the charge pump PLL loop contributes to its phase noise of PLL [11]. The simplified linear model of phase noise is shown in Fig. 3. It contains a charge pump phase frequency detector (PFD&CP) with gain of K_{pfd}, a loop filter (LF) with transfer function of $F(s)$, a voltage controlled oscillator (VCO) with gain of K_{vco}, and a frequency divider (1/N) with dividing ratio of N.

The phase noise sources are presented in this model, where $\phi_{ref,n}$, $\phi_{vco,n}$ and $\phi_{div,n}$ represent the phase noise sources of the reference, the VCO and the frequency divider, respectively. Similarly, the current noise of charge pump is denoted by $i_{cp,n}$ and the voltage noise of loop filter is denoted by $v_{lf,n}$.

As shown in Fig. 3 the open loop transfer function can be expressed as

$$H_o(s) = \frac{K_{pfd} \cdot F(s) \cdot K_{vco}}{s} \tag{2}$$

The transfer function from various noise sources to the output can refer [12]. The total phase noise of PLL can be obtained by summing the output noise power from these noise sources under the assumption that these noise sources are uncorrelated. Using the transfer functions from reference [12] and sided band power spectral density (PSD) of these phase noise sources, total phase noise can be expressed as [13]

$$\begin{aligned}\overline{\phi^2_{out,n}(s)} &= \overline{\phi^2_{out,ref}(s)} + \overline{\phi^2_{out,cp}(s)} + \overline{\phi^2_{out,lf}(s)} \\ &\quad + \overline{\phi^2_{out,vco}(s)} + \overline{\phi^2_{out,div}(s)} \\ &= G_L^2(s) \cdot \left(N^2 \cdot S^{\Phi}_{REF} + \frac{N^2}{K^2_{pfd}} \cdot S^{\Phi}_{CP} + N^2 \cdot S^{\Phi}_{DIV} \right) \\ &\quad + [1 - G_L(s)]^2 \cdot \left(\frac{K^2_{vco}}{s^2} \cdot S^{\Phi}_{LF} + S^{\Phi}_{VCO} \right)\end{aligned} \tag{3}$$

Where $G_L(s) = \frac{\frac{K_{pfd} \cdot F(s) \cdot K_{vco}}{N \cdot s}}{1 + \frac{K_{pfd} \cdot F(s) \cdot K_{vco}}{N \cdot s}} = \frac{H_o(s)}{N + H_o(s)}$. In equation (3), S^{Φ}_{REF}, S^{Φ}_{CP}, S^{Φ}_{DIV}, S^{Φ}_{LF}, S^{Φ}_{VCO} and denote the PSD of the reference, the charge pump PFD, the divider, the LF, and the VCO, respectively. The typical contributions of each component to the PLL phase noise is shown in Fig. 4.

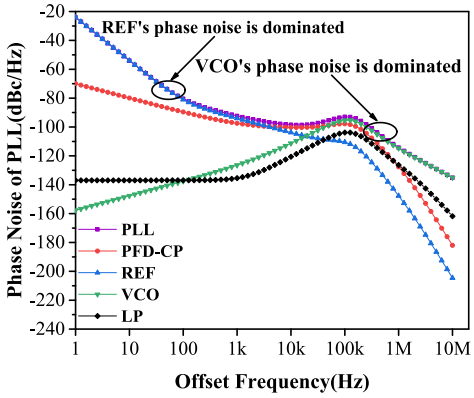

Fig. 4. The contributions of each component to PLL phase noise.

3.2 Analyzing of the impacts of loop bandwidth on SNR of MMW imaging system

In section 3.1, the contributions of each component to PLL phase noise are discussed. On the other hand, the selection of loop bandwidth also greatly has an effect on the phase noise performance of PLL frequency source and the SNR of MMW imaging system [14]. Especially, when the circuit topology of PLL frequency source is given, it's useful to optimize the loop bandwidth to obtain a high SNR of MMW imaging system.

Although we can improve the SNR of imaging system by averaging a number of measurement results in the calibration process, it's difficult to raise the SNR of mechanical scanning system due to its relatively long measure time. In general cases, the main noise source of imaging system is MMW frequency source due to its high multiplication factors [5]. Therefore, we firstly analyze the impacts of loop bandwidth on the PLL phase noise and the SNR of MMW frequency source and then derive the SNR of the imaging system with different loop bandwidths.

For practical analysis, an MMW frequency source with changeable loop bandwidth is designed and implemented. As shown in Fig. 5, the MMW frequency source is realized by multiplying the low frequency of PLL frequency synthesizer. The main components of PLL include the commercial PLL synthesizer chip ADF4106 [15], the VCO chip DCYS250500-5 [16], the active loop filter and the external crystal oscillator TCXO5300Z-10 MHz-A-V [17]. The main PLL parameters are as follows:

- Reference frequency: $f_{ref} = 10$ MHz;
- Frequency divide ratio: N = 400;
- PLL output Frequency: $f_p = 4$ GHz;
- Loop bandwidth: $B_n = 10\sim250$ kHz;

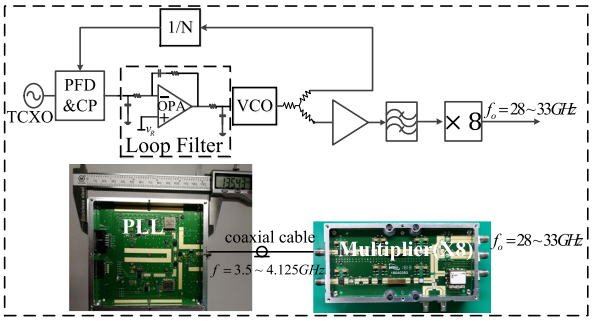

Fig. 5. The diagram and the photography of MMW frequency source.

It can be seen from Fig. 4 that the phase noise is mainly dependent on reference when offset frequency is lower than loop bandwidth. Meanwhile, outside the loop bandwidth, the noise contribution of VCO is dominated. It also can be derived from Eq. (3) that the phase noise of reference is degenerated by $20\log_{10}N$ (in this case N = 400 and the degeneration is 52 dB). In Fig. 6, the phase noise of the reference, the VCO and the PLL is described. The reference has low phase noise of −135 dBc/Hz@1 kHz and −150@10 kHz, which will have 52 dB degeneration after passing through the PLL loop. The free running VCO phase noise profile shows two different regions, which are separated by 1/f corner frequency. Below the corner frequency, it is 1/f noise region which has a slope of −30 dB/dec. When the offset frequency higher than the 1/f corner frequency, it comes into thermal noise region with a slope of −20 dB/dec [18]. The SNR of the MMW frequency source is inversely proportional to the integrated phase noise of PLL frequency synthesizer which equates to the area under the PLL phase noise profile.

As seen in Fig. 6, there is a crossover frequency at which the phase noise of degraded reference equates to the phase noise of VCO. It can be predicted that when the loop bandwidth is selected at this crossover frequency, the integrated phase noise of PLL would be minimized and the SNR of the MMW frequency source would be maximized.

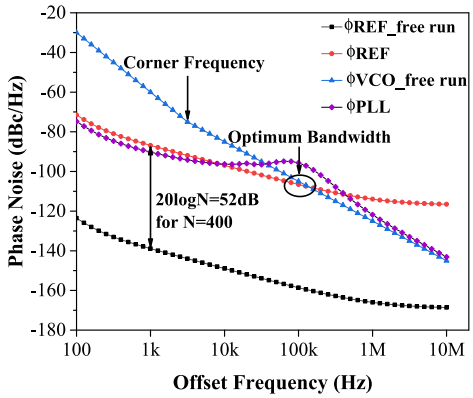

Fig. 6. The phase noise of the reference and the VCO.

The different loop bandwidths can be realized by changing the resistors and the capacitors of the loop filter. To guarantee the stability of loop, the phase margin is fixed at 46°. Taking the practical application of PLL in MMW imaging system into account, the maximal loop bandwidth of 250 kHz is selected in this experiment. In Fig. 7, the simulation and measurement results of phase noise performance at 4 GHz with different loop bandwidths are presented.

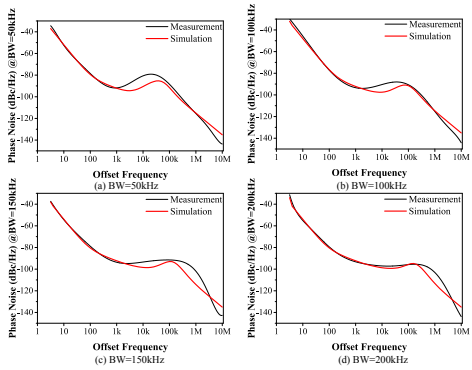

Fig. 7. The simulation and measurement results of phase noise at 4 GHz.

The MMW frequency source is achieved by multiplying the output signals of PLL frequency synthesizer. The measured phase noise of output signals of MMW frequency source at 32 GHz with different loop bandwidths is presented in Fig. 8.

The noise power of MMW frequency source at 32 GHz is achieved by integrating over the IF bandwidth of 10 MHz. Therefore, the SNR of MMW frequency source (SNR_M) can be written as

$$SNR_M = \frac{P_o}{\int_{B_I} S_{PN}(f)} \tag{4}$$

Where B_I is the IF bandwidth, $S_{PN}(f)$ is the measured phase noise of MMW frequency source at 32 GHz and P_o

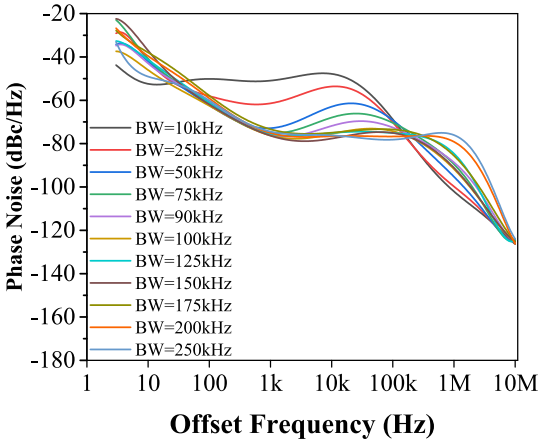

Fig. 8. The measured phase noise of MMW frequency source at 32 GHz.

is the signal power. To simplify the calculation process, we can assume that when the frequency interval is small enough, the change of phase noise between two offset frequencies is linear. Therefore, the SNR can be calculated by numerical calculation with MATLB using plenty of measurement data. Fig. 9 shows the calculated results of MMW frequency source SNR with different loop bandwidths. It can be seen that the loop bandwidth has a significant impact on the SNR of MMW frequency source and when the loop bandwidth approximately equals to the crossover frequency (100 kHz), the maximal SNR can be obtained.

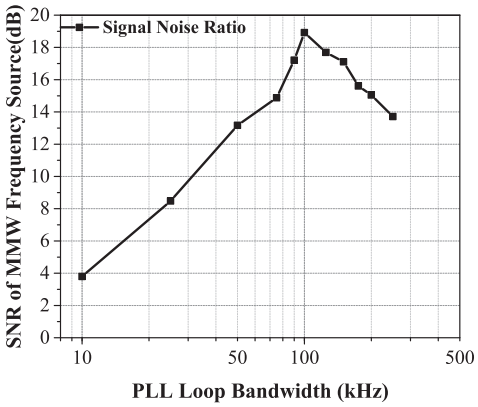

Fig. 9. The SNR of MMW frequency source with different bandwidths.

According to [5], the SNR of the imaging system can be obtained by link budget. Since the thermal noise within the IF bandwidth and quantization noise of the ADC are much lower than the phase noise of signal source, we can ignore these noises in following discussion. As shown in the Fig. 10, the path loss ($A_{FS} \cdot G_A$), the receiving gain (G_{RX}) and the IF gain (G_{IF}) have the same effects on the signal and the phase noise. Therefore, the SNR of reference LO (coupled from transmitting signal with SNR_{TX}) and the receiving RF signal (SNR_{RX}) are equal. The IF signal is achieved by mixing the reference LO and the receiving RF signal. Since the phase noise of LO and RF signal is uncorrelated, the SNR of IF signal (SNR_{IF}) will have 3 dB (NF_{MIX}) deterioration. The SNR of imaging system (SNR_S)

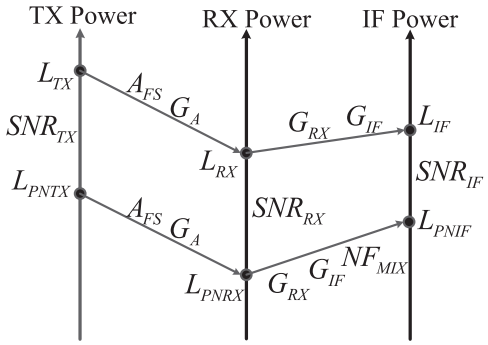

Fig. 10. The diagram of MMW imaging system link budget.

is approximately identical to the SNR of IF signal, which also equals to the SNR of MMW frequency source with 3 dB degeneration. In Fig. 10, where L_{TX}, L_{RX}, L_{IF} are the power of transmitting signal, receiving signal and IF signal, respectively. L_{PNTX}, L_{PNRX}, L_{PNIF} are phase noise of transmitting signal, receiving signal and IF signal, respectively.

Fig. 11 presents the SNR of imaging system with different loop bandwidths. The similar conclusion can be drawn that the optimum loop bandwidth of PLL for high SNR of imaging system is around the crossover frequency at which the phase noise of degenerated reference and free running VCO is identical.

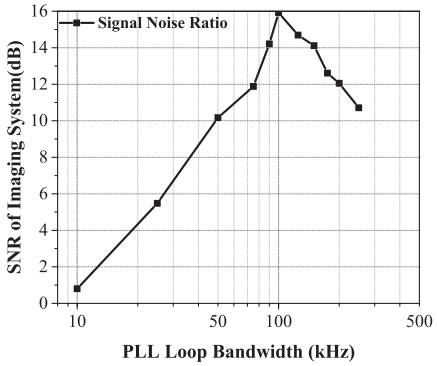

Fig. 11. The SNR of imaging system with different bandwidths.

4. The impacts of imaging system SNR on imaging performance

In order to analyze the impacts of system SNR on imaging performance, the imaging algorithm is applied to reconstruct the image. For simplifying the question, the single-frequency holographic image reconstruction is discussed. In Fig. 12, the holographic imaging system configuration is shown [19]. The MMW frequency source is posited at (x', y', z_0). Assuming that the reflection coefficient of the target at the position $(x, y, z = 0)$ is $g(x, y, z)$. The echo signal received by the receiver can be expressed as [9, 10, 20, 21]

$$f(x', y', k) = \iint g(x, y, z) \cdot \exp\left(-2jk\sqrt{(x-x')^2 + (y-y')^2 + z_0^2}\right)dxdy \quad (5)$$

Where $k = \frac{2\pi f}{c}$ is the spatial wavenumber, in this case k is a constant. Then using the transformation relationship between the sphere wave and the plane wave and the Fourier-transform relation, the image reconstruction algorithm is expressed as

$$g(x, y) = FT^{-1}_{2-D}[FT_{2-D}[f(x, y)] \cdot \exp(-jz_0k_z)] \quad (6)$$

Where $k_z = \sqrt{4k^2 - k_x^2 + k_y^2}$ and k_x, k_y, k_z are the projections of the spatial wave vector on the three coordinate axes, respectively. FT_{2-D} and FT^{-1}_{2-D} are Fourier-transform and inverse Fourier-transform, respectively.

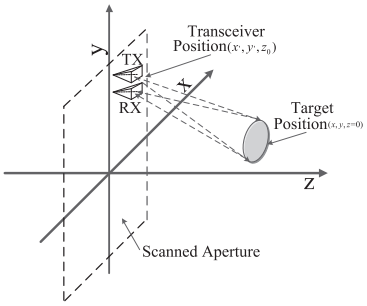

Fig. 12. The holographic imaging system configuration.

According to Eq. (5) and Eq. (6), we carry out the numerical simulation with MATLAB to validate the impacts of system SNR on imaging performance. In this simulation, the echo signal data can be generated using following equation with MATLAB codes [22]

$$f(x', y', k) = \sum\sum g(x, y, z) \cdot \frac{\exp(2jkr)}{r^2} \Delta x \Delta y \quad (7)$$

Where $r = \sqrt{(x - x')^2 + (y - y')^2 + z_0^2}$ is the distance from the ideal point target to scan aperture.

We assume that the distance r is 0.5 m and the emission frequency of MMW sources is 32 GHz. Meanwhile, the distance between two antenna elements is 5 mm and the size of the scanning aperture is 50 cm (horizontal direction) × 50 cm (vertical direction). After the target echo signal is generated by equation (7) with MATLAB, the complex white Gaussian noise is added to the original signal and the imaging system SNR is respectively set to the values which are obtained by the link budget in section 3.2.

The point spread function (PSF) simulation results of monostatic imaging with different SNR are presented in Fig. 13(a) to (d). It can be seen the higher SNR of imaging system, the lower average noise power and the better imaging performance. Therefore, choosing an optimum loop bandwidth for PLL frequency source is important to improve the system SNR and imaging quality.

The relationship between the loop bandwidth of MMW frequency source with the imaging system SNR and imaging performance is summarized in Table I.

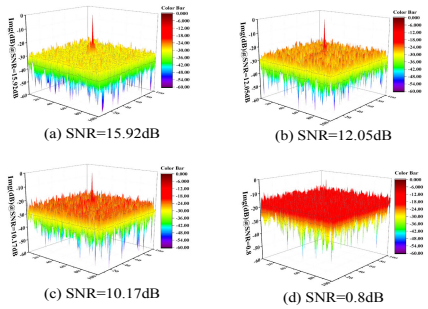

Fig. 13. The PSF simulation results of monostatic imaging.

Table I. The summarized relation between the loop bandwidth with imaging system.

B_n (kHz)	SNR_M (dB)	SNR_S (dB)	Noise (dBc)
10	3.80	0.80	−20.33
25	8.48	5.48	−24.23
50	13.17	10.17	−29.64
75	14.88	11.88	−31.43
90	17.21	14.21	−33.62
100	**18.92**	**15.92**	**−35.44**
125	17.69	14.69	−34.05
150	17.12	14.12	−33.63
175	15.61	12.61	−31.86
200	15.05	12.05	−31.33
250	13.71	10.71	−30.07

5. Conclusion

The impacts of loop bandwidth of PLL frequency source on the imaging quality have been obtained by practical measurement and numerical simulation in this paper. Simulation and experimental results demonstrate that the maximal SNR of imaging system and the highest imaging performance can be achieved by optimizing the loop bandwidth. The optimum loop bandwidth is approximately at the crossover frequency where the phase noise of degenerated reference and the free running VCO are identical. Meanwhile, when we chose the loop bandwidth of PLL frequency source, we should also make a tradeoff between the SNR, the locked time and other parameters for optimum performance in imaging system. This crossover frequency is a good starting point to select the loop bandwidth for PLL frequency source in MMW imaging system.

Acknowledgment

This work is supported by the Nation Natural Science Foundation of China under contracts Nos. 61671439 and Nos. 61731021.

References

[1] S. S. Ahmed, *et al.*: "Fully electronic *E*-band personnel imager of 2 m^2 aperture based on a multistatic architecture," IEEE Trans. Microw. Theory Techn. **61** (2013) 651 (DOI: 10.1109/TMTT.2012.2228221).

[2] S. S. Ahmed: "Advanced fully-electronic personnel security screening technology," EuCAP (2015) 1.

[3] D. M. Sheen, *et al.*: "Near-field three-dimensional radar imaging techniques and applications," Appl. Opt. **49** (2010) E83 (DOI: 10.1364/AO.49.000E83).

[4] H. Cheng, *et al.*: "A W-band auto-focus holographic imaging system for security screening," IEICE Electron. Express **14** (2017) 20170347 (DOI: 10.1587/elex.14.20170347).

[5] A. Schiessl, *et al.*: "Hardware realization of a 2 m × 1 m fully electronic real-time mm-wave imaging system," EUSAR (2012) 40.

[6] S. S. Ahmed, *et al.*: "A novel fully electronic active real-time imager based on a planar multistatic sparse array," IEEE Trans. Microw. Theory Techn. **59** (2011) 3567 (DOI: 10.1109/TMTT.2011.2172812).

[7] D. M. Sheen, *et al.*: "Wide-bandwidth, wide-beamwidth, high-resolution, millimeter-wave imaging for concealed weapon detection," Proc. SPIE **8715** (2013) 871509 (DOI: 10.1117/12.2016132).

[8] V. F. Kroupa: *Phase Lock Loops and Frequency Synthesis* (John Wiley & Sons, England, 2003) 275.

[9] Y. Zhu, *et al.*: "Practical millimeter-wave holographic imaging system with good robustness," Chin. Opt. Lett. **14** (2016) 101101 (DOI: 10.3788/COL201614.101101).

[10] D. M. Sheen, *et al.*: "Three-dimensional millimeter-wave imaging for concealed weapon detection," IEEE Trans. Microw. Theory Techn. **49** (2001) 1581 (DOI: 10.1109/22.942570).

[11] F. M. Gardner: *Phaselock Techniques* (John Wiley & Sons, New Jersey, 2005) 3rd ed. 370.

[12] X.-H. He, *et al.*: "Design and modelling of a low phase noise PLL frequency synthesizer," ICSICT (2006) 1571 (DOI: 10.1109/ICSICT.2006.306314).

[13] C. Hangmann, *et al.*: "Modeling and characterization of CP-PLL phase noise in presence of dead zone," NEWCAS (2014) 349 (DOI: 10.1109/NEWCAS.2014.6934054).

[14] K. Lim, *et al.*: "A low-noise phase-locked loop design by loop bandwidth optimization," IEEE J. Solid-State Circuits **35** (2000) 807 (DOI: 10.1109/4.845184).

[15] Analog Devices Inc.: 6 GHz integer-N PLL (2015) https://www.analog.com/media/en/technical-documentation/data-sheets/ADF4106.pdf.

[16] Synergy Microwave Co.: Voltage controlled oscillator surface mount model: DCYS250500-5 (2008) https://pdf1.alldatasheet.com/datasheet-pdf/view/302220/SYNERGY/DCYS250500-5.html.

[17] Dynamic Engineers Inc.: TCXO5300Z-10MHz-A-V Extended Temperature SMD TCXO https://d2f6h2rm95zg9t.cloudfront.net/56153022/TCXO5300Z-10MHz-A-V-2-1-_fd186c65-c367-4e6a-9518-c1c956596619.pdf.

[18] L. Liu and R. Pokharel: "Compact modeling of phase-locked loop frequency synthesizer for transient phase noise and jitter simulation," IEEE Trans. Comput.-Aided Design Integr. Circuits Syst. **35** (2016) 166 (DOI: 10.1109/TCAD.2015.2472018).

[19] H. D. Collins, *et al.*: U.S. Patent 5,455,590 (1995).

[20] C.-Y. Liu, *et al.*: "Towards robust human millimeter wave imaging inspection system in real time with deep learning," Prog. Electromagnetics Res. **161** (2018) 87 (DOI: 10.2528/PIER18012601).

[21] L. Qiao, *et al.*: "Exact reconstruction for near-field three-dimensional planar millimeter-wave holographic imaging," J. Infrared Milli. Terahz. Waves **36** (2015) 1221 (DOI: 10.1007/s10762-015-0207-z).

[22] J.-K. Gao, *et al.*: "A novel method for 3-D millimeter-wave holographic reconstruction based on frequency interferometry techniques," IEEE Trans. Microw. Theory Techn. **66** (2018) 1579 (DOI: 10.1109/TMTT.2017.2772862).